Indian J. Met. Hydrol. Geophys. (1977), 28, 2, 157-168

551.515 : 556.556(541)

Prediction of storm surges on the east coast of India

S. K. GHOSH

Meteorological Office, Safdarjung Airport, New Delhi

(*Received 24 September 1976*)

ABSTRACT. Nomograms to estimate peak storm surges generated by tropical cyclones impinging on the east coast of India are prepared using Jelesnianski's SPLASH (1972) model. The pre-computed nomograms accommodate fixed values for pressure drop, radius of maximum wind, vector motion of storms and offshore bathymetry.

Two sets of nomograms are presented — one for the northeast coast of India where the slope of the continental shelf is extremely shallow — the other for the remaining east coast where the slope in general is extremely steep.

A nomogram to correct the magnitude of the peak surge for tidal effects is also prepared for the notheast coast of India where the semi-diurnal tide range is large.

A method to estimate total sea level elevation along a coastal stretch by means of nomograms is given for the northeast coast of India.

1. Introduction

About 15 per cent of the world's yearly crop of tropical cyclones originate over the Bay of Bengal and the Arabian Sea (Gray 1975). Of these, the majority have their initial genesis over the Bay of Bengal and strike the east coast of India and the coast of Bangla Desh. There is much loss of life and property during the passage of these storms. The magnitude of devastations can be fathomed from the 1970 storm which caused more than 200,000 deaths in Bangla Desh (Flierl and Robinson 1972). The storm struck near Chittagong (22·0°N, 91·5°E) on 12-13 November 1970. A significant part of the damage is due to coastal high waters generated by the storms. Loss of life and valuables can be minimized by prediction of and protection against the total storm-tide (the sum of astronomical tide and storm surge) associated with individual storms. Estimates of storm-tide potential are valuable for efficient administration of cyclone mitigation plans, to determine the economics of coastal constructions and installations, and to determine zoning regulations to control use of land subject to extensive flooding.

Predictions of astronomical tides are available in tide tables. It is, therefore, necessary to evolve a method for the prediction of storm surges. The present study deals in part with a procedure to objectively estimate peak storm surges on the east coast of India.

2. Method for estimating the peak surge

The peak surge depends predominantly on the central pressure of a storm (Conner *et al.* 1957). There are two other important parameters which vary the peak surge significantly; they are bathymetry and vector storm motion (Jelesnianski 1972). He also found the radius of maximum wind and the coriolis parameter play only a minor role in altering the peak surge.

In order to develop an objective forecasting scheme for the peak surge, Jelesnianski (1972) used a dynamic model (1967) to compute the peak surge by changing one parameter at a time while keeping the others fixed. Instead of central pressure, he, however, chose to use the pressure drop, $\triangle P = P_{00} - P_0$, where P_{00} is the ambient pressure (in mb) and P_0 the central pressure (in mb).

The same method has been followed in the present study. The pressure drop is the most important parameter. So, computations at first are made for a range of $\triangle P$. The other parameters, *viz.*, bathymetry, vector storm motion, and storm size are fixed. To keep bathymetry and vector storm motion the same in a general sense, we initially use the concept of "standard basin" and "standard storm motion" the definitions of which are given below.

Standard basin — A basin with a straight coast line in which the depth profile sea-ward has a

TABLE 1

Geographical locations of basin centres

Basin	Lat. (°N)	Long. (°E)	Basin	Lat. (°N)	Long. (°E)
1	10°30′	79°52′	21	17°23′	82°48′
2	10 52	79 51	22	17 35	83 12
3	11 15	79 51	23	17 56	83 30
4	11 39	79 46	24	18 12	83 54
5	12 01	79 52	25	18 28	84 15
6	12 21	80 05	26	18 47	84 33
7	12 43	80 14	27	19 12	84 51
8	13 05	80 18	28	19 30	85 14
9	13 29	80 18	29	19 42	85 36
10	13 51	80 14	30	19 50	86 00
11	14 14	80 08	31	19 59	86 24
12	14 36	80 10	32	20 17	86 42
13	14 58	80 04	33	20 36	86 54
14	15 28	80 12	34	21 00	86 53
15	15 52	80 34	35	21 23	87 00
16	15 59	81 10	36	21 34	87 23
17	16 21	81 30	37	21 36	87 47
18	16 23	81 54	38	21 33	88 12
19	16 36	82 18	39	21 31	88 37
20	17° 06′	82° 24′	40	21°36′	89°02′

one-dimensional constant slope.The basin can be considered a hypothetical mean for all basins.

Standard storm motion — A storm motion with a constant speed and a track normal to the coast from sea to land. The storm must move onto land. This motion, after the speed is fixed, can be considered a hypothetical mean for all motions.

In order to compute a preliminary estimate, S_p, of the peak surge, the first step is to allow storms to traverse the standard basin, with standard motion, with the same radius of maximum wind, R (in km) and with landfall at the same latitude; each storm has different $\triangle P$. In the second step, the same storms are used but with a different R. The storms compute data to form a nomogram of peak surge against $\triangle P$ for different R.

Thirdly, the bathymetry is changed and a storm with fixed parameters traverses it. To study changing bathymetry, a coastline is divided into small segments and the mean bathymetry of each segment is set into individual basins. From marine coastal charts, the bottom topography for each segment are worked out. Then computations are made with these depth values for each basin in place of the standard basin. The non-dimensional ratios of the computed values of the peak surge to that of the standard basin gives a shoaling factor F, for each basin. A plot of these factors along the coast constitutes the second nomogram.

To correct for the effect of a non-standard storm track, several directions of motions and speeds of storms are considered whereas all the other parameters are fixed. A standard basin is used. Different values of peak surge are computed for different directions and speeds. These values are then normalized by taking the ratio of these to that generated by a standard motion. These ratios give motion factors, F_M. A polar diagram depicting isopleths of the motion factors is the third nomogram. The rays are direction, the circles are storm speed.

The product of S_p, F and F_M obtained from the first, second and the third nomograms respectively gives the final estimate of the peak surge.

3. Computations for the east coast of India

The method outlined above was used to compute potential peak surge values on the east coast of India. As few storms landfall south of 10°N, the east coast of India north of 10°N was considered in the present study.

The east coast of India north of 10°N was divided into a total number of 40 segments each of length approximately 40 km. Basins were then constructed with the mid point of each segment as a basin centre. The geographical locations of the basin centres with their numbers are given in Table 1. Each basin is 960 km long and 115 km wide. Fig. 1 illustrates the disposition of contiguous basins along the Indian coast. If A and P are two neighbouring basin centres (40 km apart), then ABCDEA and PQRSTP are rectangular basins simulating the off-shore shelf. The depths in the basins are one-dimensional and valid only at basin centre. The dynamic effects from two-dimensional bathymetry and curved coastlines are not accounted for; it is assumed these effects are small compared to the peak surge.

While working out the bottom topography of the basins, datum was changed to MSL by adding on ½ the Indian Spring tide range to the depth contours, as the soundings are reduced to Indian Spring Low Water in the marine charts.

The first step was to construct a standard basin. An examination of the depth profiles revealed dramatic differences in their patterns north and south of 20·5°N. The bathymetry south of 20·5°N is extremely steep and to its north is extremely shallow. It was, therefore, felt necessary to construct standard basins separately for the two regions.

Two standard basins — one a mean basin for the basin centres 1 to 33 and the other for 34 to 40 — were accordingly constructed and computations of peak surge were made for each separately.

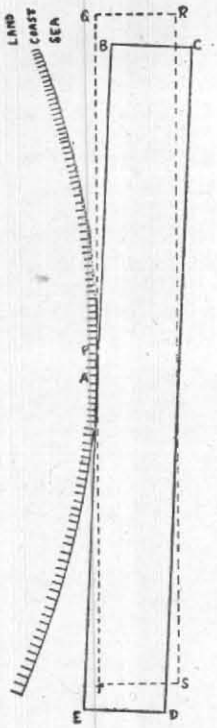

Fig. 1. Rectangular basins, 960 km long and 115 km wide, with two neighbouring coastal points A and P, 40 km apart, as basin centres

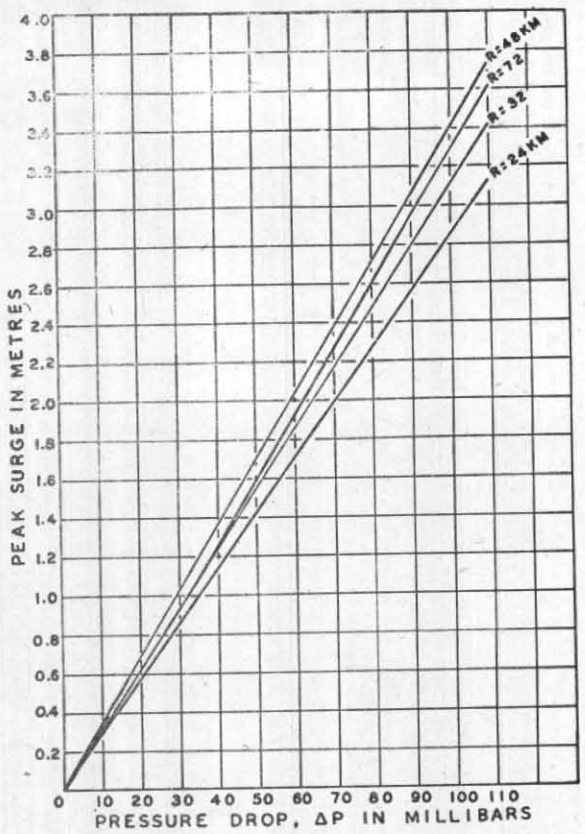

Fig. 2. Nomogram at peak surge on the open coast as a function of pressure drop and radius of maximum winds for the southeast coast of India

3.1. *Computations for Basins 1 to 33*

3.1.1. *Preliminary Estimate*

The standard basin for the basins 1 to 33 is a one-dimensional depth profile of 6 m at the coast and a constant slope of 2·25 m per km.

The standard motion is taken as a storm speed of 24 kmph and a track normal to the coast from sea to land.

The first nomogram which gives a preliminary estimate of the peak surge was constructed by changing $\triangle P$ and R and is reproduced as Fig. 2. For constant R, each curve is nearly a straight line passing through the origin. So, if δp is the error in the pressure drop $\triangle P$, then the estimated peak surge has an error of $\delta p/\triangle P$. Thus, a 2-mb error in pressure drop of 50 mb results in an error of 4 per cent in the peak surge.

An examination of Fig. 2 reveals that the peak surge is weakly or mildly dependent on R according as $\triangle P$ is small or large. For example, the difference between the peak surge values for storms of R=24 and 48 km is 0·44 m when $\triangle P$=80 mb whereas it is 0·10 m when $\triangle P$=20 mb. Again, for constant $\triangle P$, the peak surge reaches its maximum value for R nearly equal to 50 km. This means that there is a critical storm size which generates maximum peak surge in a standard basin for a standard storm motion.

3.1.2. *Corrections for Bathymetry*

As has already been stated, the basin centres were 40 km apart. The depth profile at each basin centre and at distances of 10 and 20 km on either side of the basin centre, were plotted and the mean of the five profiles was taken to represent the bottom topography of the basin in question. As there were 33 segments, 33 basins with different depth profiles were obtained. These basins were input into the surge model in order to compute the peak surges for the effect of varying bathymetry along the coast. The second nomogram was thus constructed and is presented in Fig. 3. In this figure, the vertical lines are nearly 100 km apart on the coast. Coastal cities are shown along the abscissa. The ordinate gives the shoaling factor, F_{SE} (ratios of peak surge relative to a standard basin). The factors are for the open coast peak surge. It is seen from the figure that the coast near Nagapatam, the segment of about 100 km width near 50 km south of Masulipatam and the

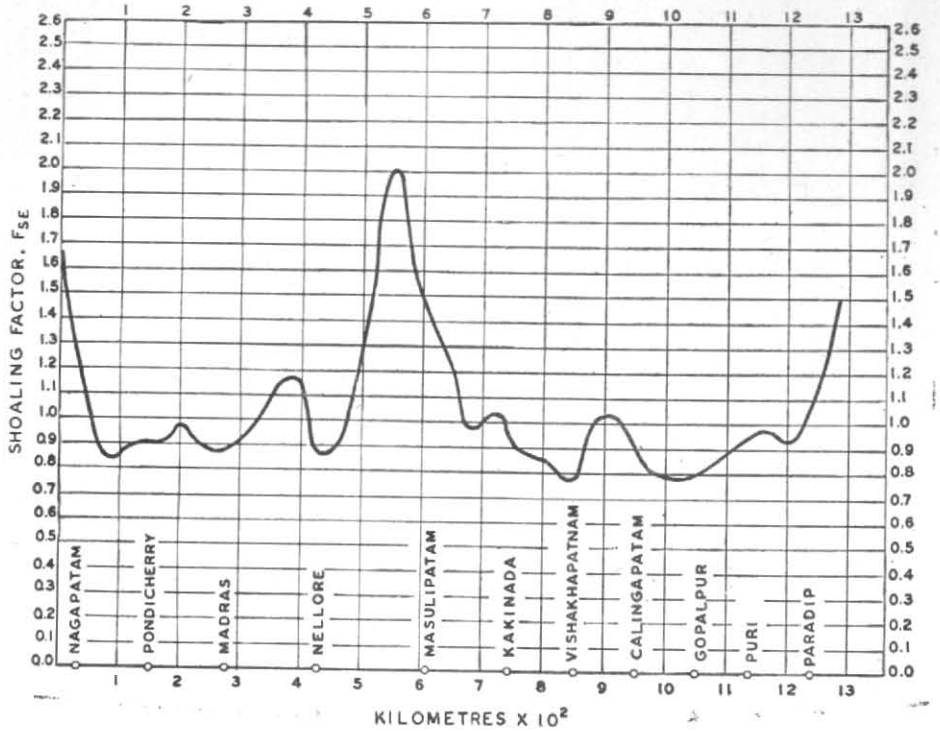

Fig. 3. Nomogram for shoaling factors for the southeast coast of India

the coast east of Paradip have high potentials of peak storm surge.

It may be mentioned that the figure is for R=48 km, $\triangle P$= 38 mb and standard storm motion. When these parameters are changed, shoaling factor F_{SE}, is likely to change but only by a small degree. While preparing the shoaling curve, the change in the coriolis parameter with latitude was taken into cosideration.

3.1.3. *Corrections for storm motion*

The vector motion of a storm has significant influence on surge generation. There exists a critical vector storm motion relative to a coast that gives the highest surge, all other parameters remaining the same (Jelesnianski 1972). The critical speed is generally greater than 50 kmph. Landfalling storms rarely attain a critical speed; as such, it was not considered in the present study.

The third nomogram was prepared to correct for the effect of different vector storm motions on coastal surges. The isopleths of the correction factors are given in Fig. 4. The figure gives the motion factor, F_M, for R=48 km, $\triangle P$=38 mb, latitude= 15° N and standard basin. If we change these parameters F_M varies but only slightly. The angle of the storm's track relative to the coast, θ, is defined in the top right corner of the figure. In this, the observer faces the land from the sea. On the coast to his right is relative north, *i.e.*, 0° and to his left is relative south, *i.e.*, 180°. The angle θ is measured clockwise from shore to track where the track terminates at the landfall point. From the figure it is clear that landfalling storms produce higher peak surges for the same speed than exiting (land to sea) storms. For landfalling storms the peak surge increases with increasing storm speed. For exiting storms, however, the opposite is true, *viz.*, the peak surge decreases with increasing storm speed. Also, the peak surge is maximum when θ is between 70° and 80°, other parameters remaining constant.

The figure is speculative for storms crossing the coast with a small acute angle (*viz.*, for θ=150° to 210° and θ=330° to 030°).

3.1.4. *Final estimate of the peak surge and the total storm-tide*

The product of S_p, the preliminary estimate, F_{SE}, the shoaling, factor, and F_M, the motion factor, as obtained in the previous sections gives the final estimate of the peak surge. This is to be superimposed with astronomical tide at the time of landfall to obtain the total storm-tide.

3.1.5. *Dependence of peak surge on maximum wind*

For tropical storms, the generated surge due to wind stress is much greater than that due to pressure

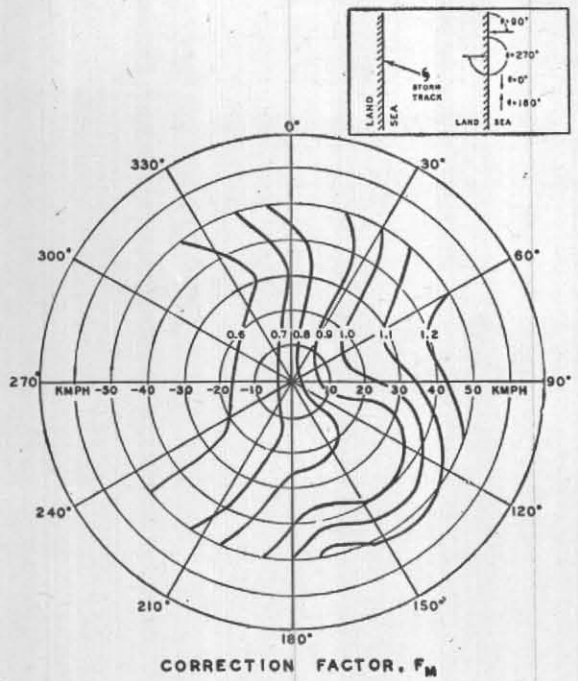

Fig. 4. Nomogram of correction factors for vector storm motion for the southeast coast of India. Radii are storm speeds and rays are crossing angles of storm track to the coast, θ. Radius of maximum wind, 48 km

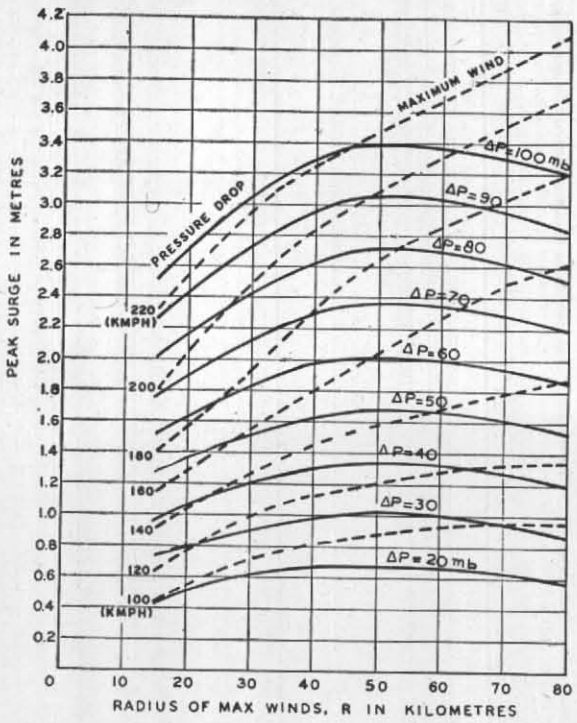

Fig. 5. Nomogram relating peak surge with radius of maximum wind, pressure drop and maximum wind for the southeast coast of India

gradient force. One is, therefore, inclined to believe that the peak surge decreases (increases) with decreasing (increasing) maximum wind. This, however, is not necessarily true as shown in Fig. 5 which relates R, $\triangle P$, W_M and the peak surge, where W_M is the maximum wind. From the figure it is clear that the same W_M can produce significantly different peak surges for various values of $\triangle P$ and R. For example, a 200 kmph maximum wind produces 1·8 and 3·7 m of peak surge when R runs from 15 to 80 km respectively. Again, a 180 kmph maximum wind produces 1·74 and 3·20 metres of peak surge when $\triangle P$ runs from 60 to 100 mb respectively. Thus an accurate determination of maximum wind alone does not guarantee a correct estimate of peak surge. It may be noted that Fig. 5 is no more than Fig. 2 in different format. In Fig. 5, R stands out; in Fig 2, $\triangle P$ stands out. It may also be pointed out that the maximum wind as depicted in the nomogram was derived from an idealized wind profile and is not the same as the maximum wind obtained from synoptic observations. The latter is about 1·3 times the former (Jelesnianski 1972).

From Fig. 5 it is also apparent that when $\triangle P$ is constant, the peak surge increases with R until a critical value of R is reached (in the present case, critical R=52 km) and then decreases with increasing R. But when W_M is constant, the peak surge increases progressively with R.

3.2. *Computations for basins 34 to 40*

3.2.1. *Preliminary estimate*

The standard basin for the basin numbers 34 to 40 has a depth of 4·5 m at the coast and a constant slope of 0·28 m per km.

The standard motion is taken as a storm speed of 25 kmph and a track normal to the coast from sea to land.

The preliminary estimate, S_p', of the peak surge is given by Fig. 6. As in the previous case, each curve is nearly a straight line passing through the origin for the same R. Again, the peak surge is mildly or weakly dependent on R according as $\triangle P$ is large or small. For constant $\triangle P$, the peak surge attains its maximum at R nearly equal to 50 km.

A comparison of Fig. 6 with Fig. 2 shows much higher peak surge for the northeast standard basin. This is because the basin is very shallow compared to the other basin and the peak surge is inversely related to the steepness of the basin (Jelesnianski 1972).

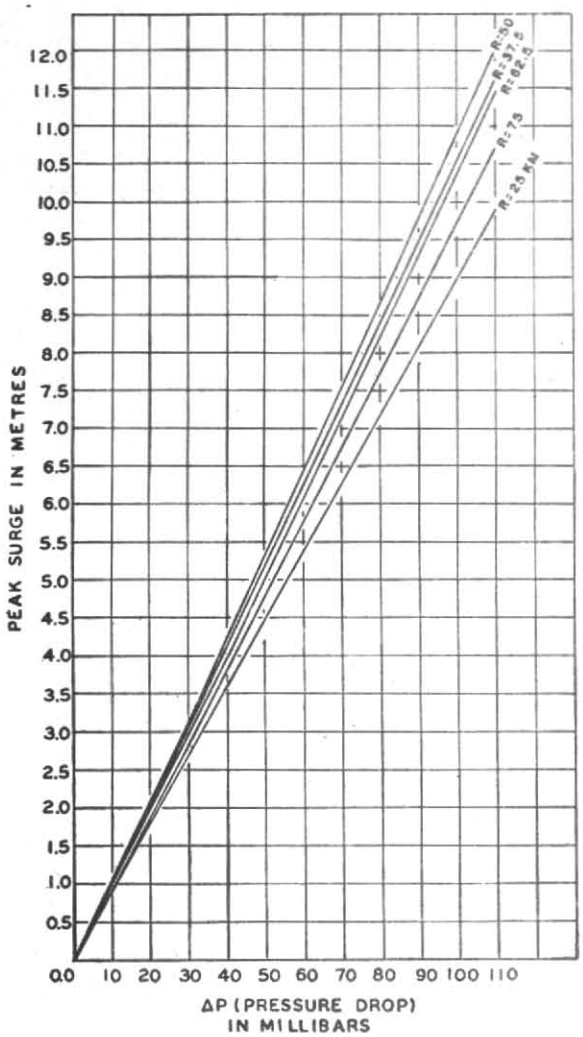

Fig. 6. Nomogram of peak surge as a function of pressure drop and radius of maximum winds for the northeast coast of India

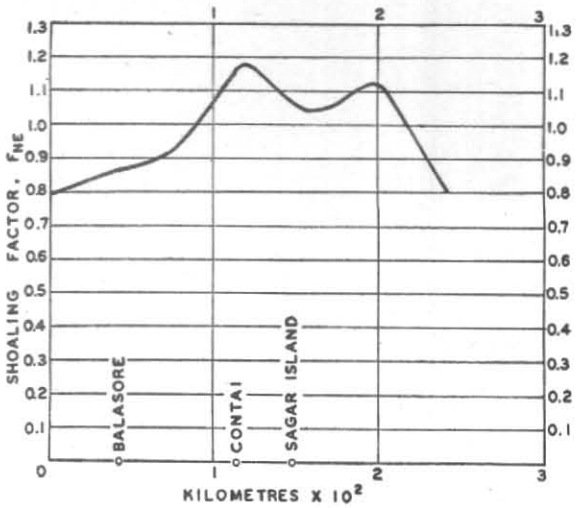

Fig. 7. Nomogram for shoaling factors for the northeast coast of India

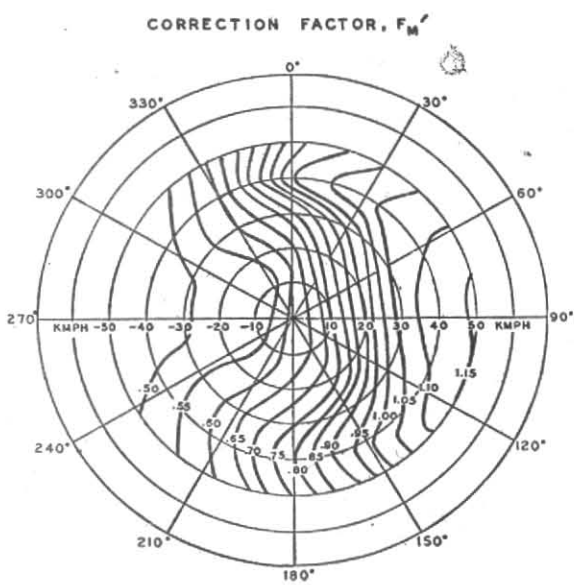

Fig. 8. Nomogram of correction factors for vector storm motion for the northeast coast of India. Radii are storm speeds and rays are crossing angles of storm track to the coast, θ. Radius of maximum wind, 50 km

3.2.2. *Corrections for Bathymetry*

The correction factors to be applied on account of changing bathymetry of the individual basins are given in Fig 7. As in Fig. 3, the vertical lines are nearly 100 km apart and important coastal landmarks are shown along the abscissa. The ordinate gives the shoaling factor, F_{NE}. It appears from the figure that the whole of the West Bengal coast and adjoining Orissa coast are susceptible to high storm surges, the most being the segment near the town of Contai.

3.2.3. *Corrections for storm motion*

The isopleths of correction factors for different vector storm motions are shown in Fig. 8. The angle of the storm's track θ has the same meaning as stated in section 3·1·3. As in the previous case, landfalling storms produce higher peak surges than exiting storms. Also, the peak surge increases (decreases) with increasing storm speed for landfalling (exiting) storms. The high gradient of isopleths in Fig. 8 indicates that for landfalling storms the peak surge increases *rapidly* with storm speed when the speed is between 10 and 30 kmph and θ is between 30° and 150°. It may also be seen from the figure that the peak surge is maximum when θ is between 80° and 90°, other parameters remaining the same. The motion factors F_M' as given in the figure were computed for $\triangle P = 50$ mb, $R = 50$ km and latitude $= 20°$N and are liable to change, although slight, when the parameters are changed. The

figure, just as Fig 4, is speculative for storms crossing the coast with a small acute angle.

3.2.4. *Final estimate of the peak surge*

The product of S_p', the preliminary estimate, F_{NE}, the shoaling factor and $F_{M'}$, the motion factor, as obtained in the previous sections gives the final estimate of the peak surge.

3.2.5. *Dependence of peak surge on maximum wind*

As in Fig. 5 of the previous case, Fig. 9 gives the inter-relations of R, $\triangle P$, W_M and the peak surge. As before, only two of the parameters are to be specified to determine the other two. The peak surge is, however, valid only in the standard basin for the standard motion. In this case also, when $\triangle P$ is constant, the peak surge increases with R till R=48 km and then decreases with increasing R. But when W_M is constant, the peak surge increases progressively with R.

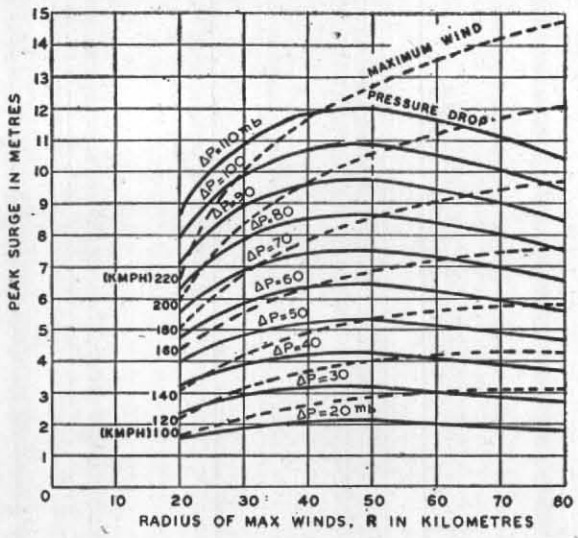

Fig. 9. Nomogram relating peak surge with radius of maximum wind, pressure drop and maximum wind for the northeast coast of India

3.2.6. *Total sea level elevation due to astronomical tide and storm surge*

The spring range of astronomical tide, defined as the average semi-diurnal range occurring semi-monthly as the result of the moon being new or full, varies between 1·9 and 4·8 m on the north Orissa and West Bengal coasts with the maximum of 4·8 m near the mouth of the *Hooghly* river (U.S. Department of Commerce *Tide Tables*). Because of such a large range of tide, the total sea level elevation would significantly differ depending on which phase of the tidal cycle landfall occurs. For example, if landfall occurs at the time of high (low) tide, one is inclined to estimate the total sea level elevation by adding (subtracting) the tide to (from) the surge. But, as pointed out by Das *et al.* (1974), mere superposition does not always provide a correct estimate because of tide-surge interaction. In order to obtain a somewhat realistic value of the total tide, a simple method was adopted in the present study.

It was assumed that a value for tide was present throughout the basin and during the whole duration of movement of the storm. Thus water level in the whole basin was raised to a new datum by an amount equal to the tide. Computations were made with the standard basin and standard motion by increasing the quiescent water levels throughout a basin, ranging by an amount of half the largest spring range, *viz.*, 2·4 m at the *Hooghly* river. Because of increase in depth values, the computed surge was lower than that without tide. This value, if added to the maximum high tide may be an underestimate for the total sea level elevation since a fixed tide value would never be present throughout the basin for the duration of the storm motion. On the other hand, if tide is merely added to the surge (computed without any alteration of the sea level due to tide), it gives an overestimate of the total sea level elevation (Das *et al.* 1974). Therefore, a correct estimate presumably lies between the two extreme estimates. In the present study the mean of the two estimates was taken as a realistic measure of the total sea level elevation. When the tide is subtracted from this value, we get the corrected surge. The percentage of corrected surge to the computed surge (without tide) was called the correction term for surge, S_T.

Computations were made for a standard storm and basin for the northeast coast, for different pressure drops, *viz.*, 20, 30, 40, 50 and 60 mb and for tides upto $\pm$2·4 m. The computed values were then plotted against the non-dimensional factors of tide/surge to obtain a diagram for surge correction. As the curves were different for different pressure drops, the abscissa was normalized by a factor of $\triangle P/40$ to obtain a curve independent of $\triangle P$. This resulted in the separate curves being nearly coincident. The mean of these curves is shown in Fig. 10 which is the nomogram for the surge correction term for tides.

To use this nomogram, tide value at the point and time of landfall is to be obtained from tide tables. Peak surge is then to be found out by the product of S_p', F_{NE} and $F_{M'}$ obtained by using the first three nomograms. Fig. 10 is then to be entered with the ratio of tide/surge $\times \triangle P/40$ on the

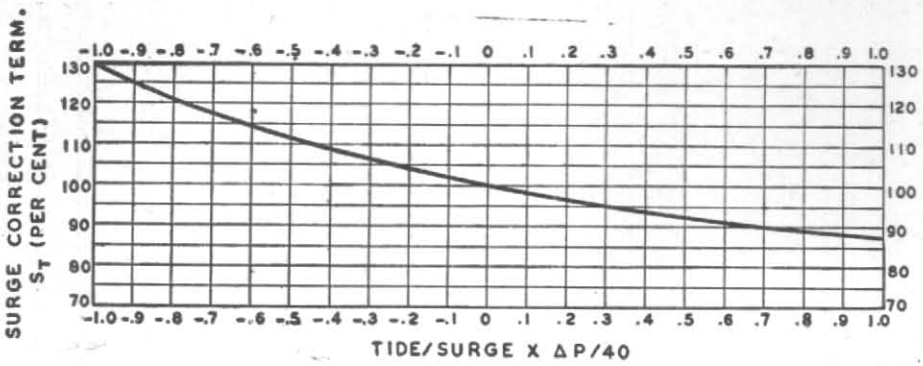

Fig. 10. Nomogram of surge correction term for the northeast coast of India

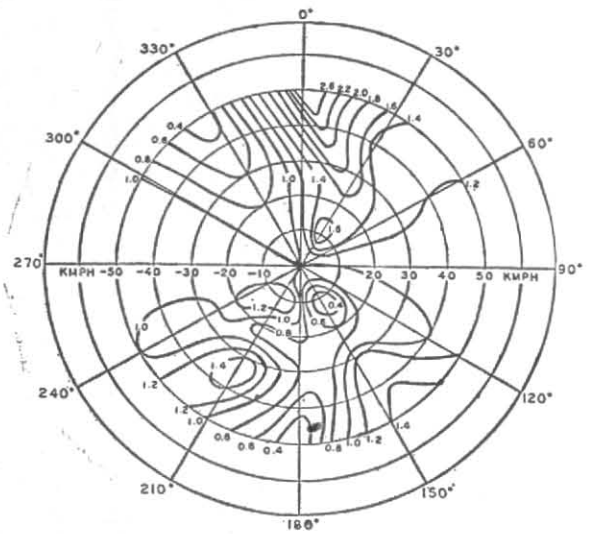

Fig. 11. Isopleths of D_1/R, D_1 being the distance from landfall position to point of peak surge on the coast and R the radius of maximum wind. Radii are storm speed and rays are crossing angles of storm track to the coast. Landfall point is the origin

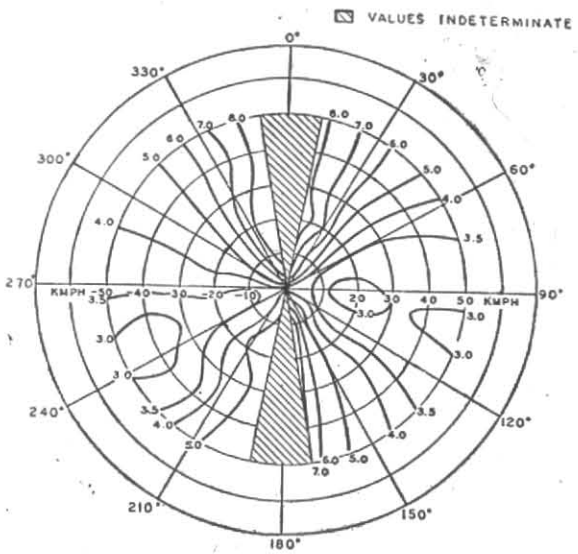

Fig. 13. Same as Fig. 12, but for 1/4 peak surge value

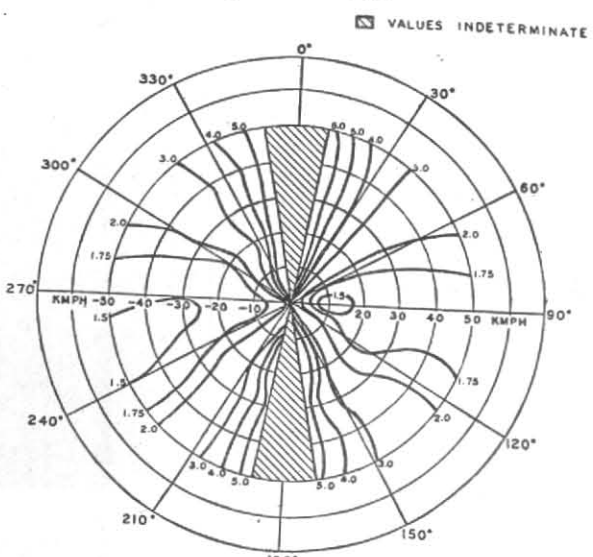

Fig. 12. Isopleths of D_2/R, D_2, being the distance on the coast from point of peak surge to point on coast having 1/2 the peak surge to the right of landfall. Arguments same as Fig. 11. Position of peak surge is the origin

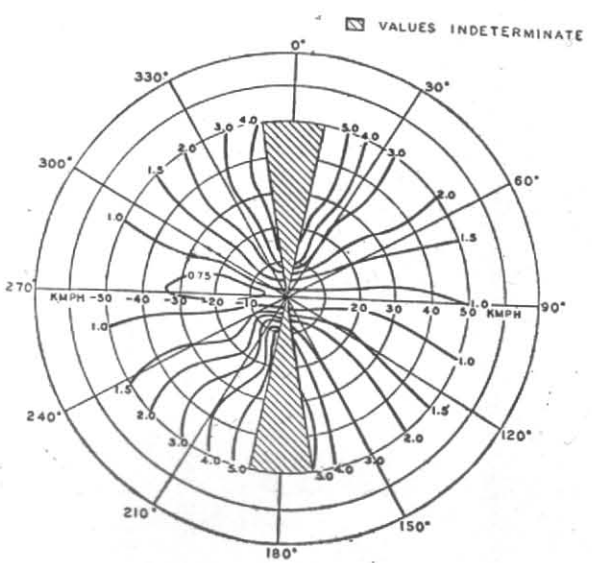

Fig. 14. Same as Fig. 12, but to left of landfall

abscissa. Correction term S_T is to be read off from the corresponding ordinate of the curve. To obtain the total sea level elevation the value of the tide is to be added (subtracted) to (from) the product of S_T (expressed as a fraction) and the peak surge if the tide is high (low). For example, if surge =4 m, tide=2m and $\triangle P$=40 mb, we have tide/surge $\times$ $\triangle P/40$ = 2/4 $\times$ 40/40=0·5. From Fig. 10, we get surge correction term= 93% or 112% according as tide is high or low. So the corrected surge is 4 $\times$ 0·93=3·72 m if tide is high or 4 $\times$ 1·12=4·48 m if tide is low. Therefore, the total sea level elevation is 3·72+2 = 5·72 m or 4·48—2=2·48 m according as tide is high or low. A superposition of surge and tide would give 6 m if tide is high and 2 m if tide is low.

3.2.7. *Envelope of storm tide*

An estimate of the highest sea level elevation or peak storm tide gives the high water for only one point on the coast affected by a storm. It is desirable to determine the envelope of storm tide along the coast. A method to do this is described below.

For the northeast coast of India, nomograms (Figs. 11 to 15) were prepared based on pre-computed surge envelopes (curves of maximum surge along the coast) generated by the standard storm moving across the standard one-dimensional basin (These were made for the northeast coast, not for the remaining east coast of India). Fig. 16 illustrates a typical coastal surge envelope for a landfall storm. In this figure, L, P, H_R, Q, H_L and O are respectively the landfall point, the point of peak surge, the point at which 1/2 peak surge occurs to the right of landfall, the point at which 1/4 peak surge occurs to the right of landfall, the point at which 1/2 peak surge occurs but to the left of landfall and the point of zero surge. Let D_1 be the distance to point of peak surge on the coast from landfall and D_2, D_3, D_4 and D_5 the distances from point of peak surge to point on the coast having 1/2 peak surge to the right of landfall, having 1/4 peak surge to the right of landfall, having 1/2 peak surge to the left of landfall and having zero surge. Then, in Fig. 16, LP=D_1 $PH_R=D_2$, PQ=D_3, $PH_L=D_4$ and PO=D_5. If A, B, C and D are the points on the vertical lines through H_L, P, H_R and Q respectively so that PB = the peak surge, $H_RC = H_LA = \frac{1}{2}$ PB and QD=1/4 PB, then the curve OABCD is a surge envelope.

Figs. 11 to 15 provide D_1 to D_5. These nomograms contain isopleths of D_1/R, D_2/R, D_3/R, D_4/R and D_5/R. Distances were normalized so as to make them independent of R. In the nomograms rays are crossing angles of storm track to the coast and radii are storm speeds.

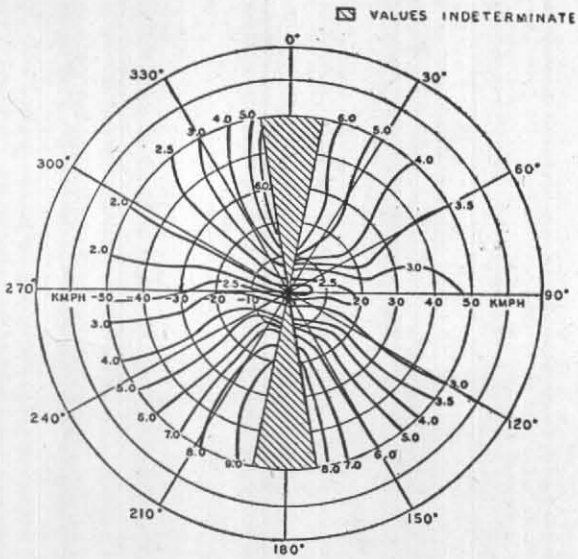

Fig. 15. Same as Fig. 12, but for zero surge

By using the above nomograms we can construct the envelope of storm tide for landfall storms. To illustrate how this can be done, let L (Fig. 17) be the landfall position of a storm. From Figs. 11 to 15 we obtain D_1, D_2, D_3, D_4 and D_5 and mark the points P, H_R, Q, H_L and O on the coast so that LP=D_1, $PH_R=D_2$, PQ=D_3, $PH_L=D_4$ and PO=D_5. From Figs. 6, 7 and 8 we obtain the value of the peak surge. While using Fig. 7, shoaling factor corresponding to point P is to be taken. On the vertical line through P we mark B, so that PB=the peak surge. We mark points A, C and D on the vertical lines through H_L, H_R and Q so that $H_LA=H_RC=1/2$ PB, and QD=1/4 PB. The curve OABCD is a surge envelope for a one-dimensional depth basin, with the depth profile offshore from P. However, shoaling factors at H_L H_R and Q are usually different from that at P. So, in order to obtain the maximum surge at H_L, H_R, and Q we have to make shoaling corrections for these points. From Fig. 7, we obtain the shoaling correction factors at H_R, divide by the shoaling factor at P and then multiply this ratio with 1/2 peak surge to get the corrected maximum surge at H_R. We mark the point C_1 on H_RC so that H_RC_1 = the corrected maximum surge at H_R. Similar procedure is adopted to obtain the point A_1 and D_1 on H_LA and QD respectively. The curve $OA_1BC_1D_1$ is the surge envelope corrected for shoaling.

Next we correct for tidal effect. From Fig. 10, we obtain the peak surge corrected for interaction with tide. We mark B_2 on PB so that PB_2=the peak surge corrected for tide interaction. Again we enter Fig. 10 with surge = H_RC_1 and obtain the surge corrected for tide interaction for the point H_R. Let this be equal to H_RC_2 where C_2 is a point

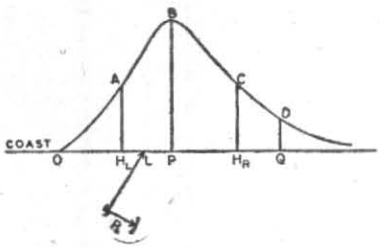

Fig. 16. A coastal surge envelope in the vertical. The storm track is in the horizontal

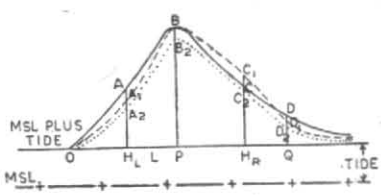

Fig. 17. An envelope of storm tide (high tide)

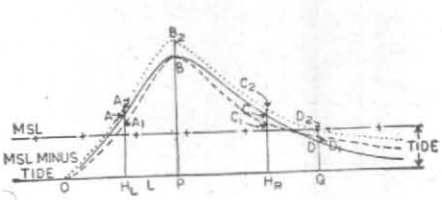

Fig. 18. An envelope of storm tide (low tide)

$LP=D_1$, $PH_R=D_2$, $PQ=D_3$, $PH_L=D_4$, $PO=D_5$ $H_RC=\frac{1}{2}$ $PB=H_LA$, $QD=\frac{1}{4}$ PB

——— OABCD : Surge envelope without shoaling correction
– – – $OA_1BC_1D_1$: Surge envelope with shoaling correction
. . . $OA_2B_2C_2D_2$: Surge envelope with tidal effect

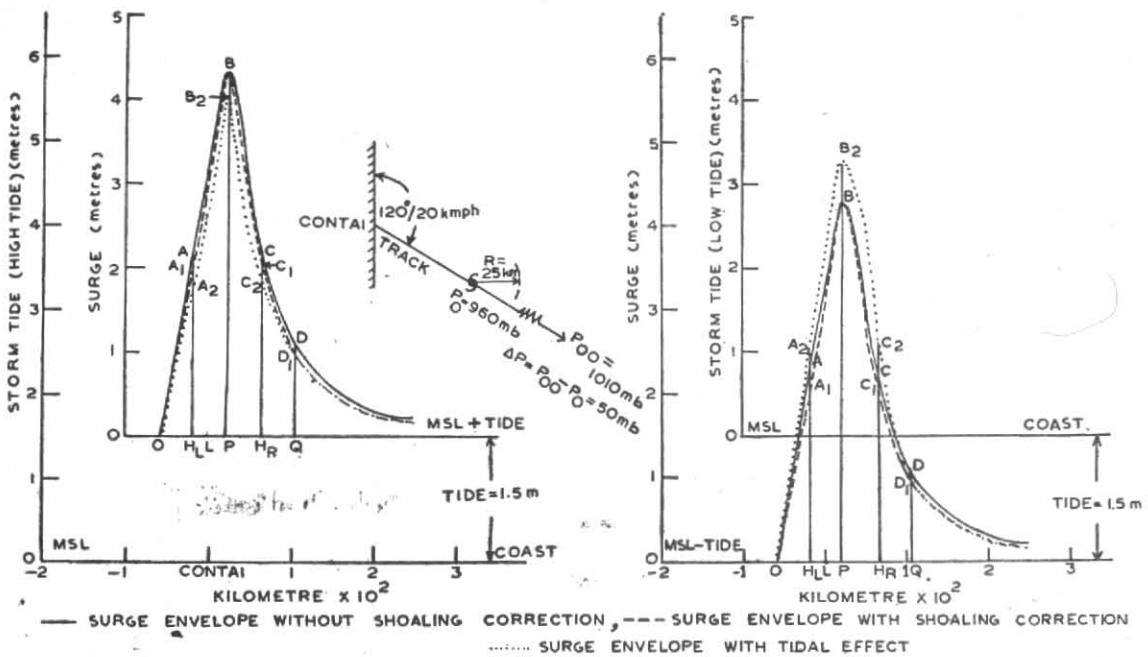

Fig. 19. A storm tide envelope for given storm parameters and tide (high tide)

Fig. 20. A storm tide envelope for given storm parameters and tide (low tide)

on H_RC. Similarly we mark A_2 and D_2 on H_LA and QD respectively. The curve OA_2 $B_2C_2D_2$ is the final surge envelope. The datum for the surge envelope is sea level, *i.e.*, MSL$\pm$tide according as tide is high or low. To obtain storm tide envelope we change the datum to MSL. With reference to this new datum, the final surge envelope becomes the envelope of storm tide. Figs. 17 and 18 illustrate storm tide envelopes for high and low tide respectively.

It is to be noted that when 1/2 surge or 1/4 surge is less than astronomical tide, Fig. 10 is not applicable. In such a case tide is merely to be superimposed on surge to obtain storm tide. Or in other words surge is not to be corrected for interaction with tide.

In each of the Figs. 12 to 15, a cut-out of 10 degrees on either side of the coast from the landfall point is marked. In the cut-out, values are indeterminate. This is because every point on the coast has the same peak surge when a storm moves up or down the coast. As such, D_2, D_3, D_4 and D_5 cannot be determined. The argument applies to storms moving at very small angles to the coast. However, the zones of indeterminate values of D_2, D_3, D_4 and D_5, *viz.*, 10 degrees on either side of the coast were arbitrarily fixed in order that the isopleths are seen distinctly.

3·2·7·1. *Examples of storm tide envelope*

Examples are cited below to show how to construct storm tide envelopes.

Let a storm of pressure drop 50 mb and size 25 km moving at an angle of 120° relative to the coast with a speed of 20 kmph landfall at Contai (Fig. 19).

In the following, we deal with cases of high and low tide separately. In the first case we assume high tide of 1·5 m at the time of landfall and in the second low tide of the same magnitude.

Case I — High Tide

The first step in the construction of a storm tide envelope is to prepare a surge envelope without shoaling correction (*i.e.*, for one dimensional bathymetry). The procedure to do this is given below.

(a) *Surge envelope without shoaling correction*

For the example under consideration we get, from Figs. 11 to 15, D_1/R=0·87, D_2/R=1·70, D_3/R=3·30, D_4/R=1·60 and D_5/R=3·20. As, R=25km, we have D_1=(0·87×25=) 22 km, D_2=44, D_3=83, D_4=40 and D_5=80 km. Let us consider a graph with coast at a datum of MSL *plus* tide as abscissa and surge as ordinate (Fig. 19). We mark L, the landfall point, on the abscissa. Then the points P, H_R, Q, H_L and O are marked also on the abscissa so that D_1=LP =22, D_2=PH_R=44, D_3=PQ=83, D_4=PH_L= 40 and D_5=PO=80 km. From Figs. 6, 7 and 8 respectively we get S_P' = 4·50 m, F_{NE} (for point P)= 1·13 and F_M'=0·85. So the peak surge=4·50× 1·13× 0·85=4·32 m. Therefore, 1/2 peak surge= 2·16 m and 1/4 peak surge=1·08 m. We plot on ordinate 4·32, 2·16, 1·08 and 2·16 m against P, H_R, Q and H_L respectively. Let these points be B, C, D and A. Then OABCD is the surge envelope *without* shoaling correction; *e.g.*, if the depths of the sea at P were representative for all of the north-east coast, *i.e.*, 1-dimensional depths.

Next step is to construct the surge envelope *with* shoaling correction; *e.g.*, for 2-dimensional depths. To do this we proceed as follows.

(b) *Surge envelope with shoaling correction*

From Fig. 7, F_{NE} for H_R, Q and H_L is 1·08 0·98 and 1·04 with respect to a standard basin. So the corrected surge at H_R, Q and H_L is (2·16× 1·08/1·13=) 2·07, (1·08×0·98/1·13=) 0·94 and (2·16×1·04/1·13=) 1·99 m respectively. Here we are re-normalizing the shoaling curve of Fig. 7, so that the shoaling factor is unity at the point P. We plot 2·07, 0·94 and 1·99 against H_R, Q and H_L and get C_1, D_1 and A_1 respectively. Then $OA_1BC_1D_1$ is the surge envelope *with* shoaling correction. There is no shoaling correction at the point P.

We next proceed to correct for tidal effect :

(c) *Surge envelope with tidal effect*

We have tide =1·5 m and surge=4·32 m at P. So tide/surge×$\triangle P$/40=1·5/4·32 × 50/40=0·44. Entering Fig. 10 with this value on the abscissa we proceed to the curve and read off the corresponding ordinate as 93 per cent for high tide. So the corrected peak surge=4·32×0·93=4·02 m. For H_R, tide/surge × $\triangle P$/40=1·5/2·07×50/40=0·90. So, from Fig. 10, surge correction term=88 per cent. Therefore, the corrected surge at H_R=2·07 × 0·88 =1·82 m. For Q, tide=1.5 m and surge = 0·94 m. As surge is less than tide, Fig. 10 is not applicable. We, therefore, make no correction for tidal effect at Q. For H_L, tide/surge×$\triangle P$/40=1·5/1·99×50/ 40=0·94; so from Fig. 10, surge correction term= 88 per cent. Therefore, the corrected surge at H_L=1·99×0·88=1·75 m. We plot 4·02, 1·82 and 1·75 m against P, H_R and H_L and obtain B_2, C_2 and A_2 respectively. Then $OA_2B_2C_2D_1$ is the surge envelope with tidal effect.

(d) *Storm tide envelope*

In order to obtain the storm tide envelope we change the datum from MSL *plus* tide to MSL. We want to use a MSL datum because land contours are generally referred to such a datum. With reference to MSL, $OA_2B_2C_2D_1$ is the storm tide envelope.

Thus the peak storm tide is 5·52 m if the storm landfalls at the time of high tide is 1·5 m. A superposition of tide and surge would give 1·5+4·32= 5·82 m.

We next proceed to construct the storm tide envelope for the case of the same storm landfalling at the time of low tide of 1·5 m.

Case II — Low Tide

We take a graph of coast at a datum of MSL *minus* tide as abscissa and surge as ordinate. On the abscissa we mark L, the landfall point and P, H_R, Q, H and O so that D_1=LP=22, D_2=PH_R =44, D_3=PQ=83, D_4=PH_L=40 and D_5= PO=80 km (Fig. 20). We then proceed to construct the surge envelope without shoaling correction, the curve OABCD, and the surge envelope with shoaling correction, the curve $OA_1BC_1D_1$, as in the case of high tide. As the storm parameters are the same, the curves OABCD and $OA_1BC_1D_1$ in Figs. 19 and 20 are identical.

We next correct for tidal effect for low tide of 1·5 m.

(a) *Surge envelope with tidal effect*

At P, we have, tide/surge×$\triangle P$/40 = 0·44 (as in the case of high tide). From Fig. 10, we obtain surge correction term for *low* tide corresponding to this value as 110 per cent. So the corrected peak surge = 4·32×1·1 = 4·75 m. For H_R

and H_L, the surge correction term is 125 per cent and 127 per cent respectively corresponding to tide/surge $\times \triangle P/40 = 0 \cdot 90$ and $0 \cdot 94$. So the corrected surge = $(2 \cdot 07 \times 1 \cdot 25 =) 2 \cdot 59$ and $(1 \cdot 99 \times 1 \cdot 27 =) 2 \cdot 53$ m at H_R and H_L respectively. We plot 4·75, 2·59 and 2·53 m against P, H_R and H_L and get B_2, C_2 and A_2 respectively. Then $OA_2B_2C_2D_1$ is the surge envelope with tidal effect.

(b) Storm tide envelope

In order to obtain the storm tide envelope, we change the datum from MSL *minus* tide to MSL. With reference to this new datum, *viz.* MSL, the curve $OA_2B_2C_2D_1$ becomes the storm-tide envelope.

Thus the peak storm tide is 3·25 m if the storm landfalls at the time of low tide is 1·5 m. A superposition of tide and surge would give $4 \cdot 32 - 1 \cdot 5 = 2 \cdot 82$ m.

We have already seen that the peak storm tide is 5·52 m in the case of high tide. The difference of the peaks, *viz.*, $(5 \cdot 52 - 3 \cdot 25 =) 2 \cdot 27$ m is quite large. This points out the importance of correct estimate of landfall time in operational storm surge prediction.

Without the correction for tidal effect the peak storm surge is 4·32 m. Superposition of surge on tide gives the storm tide $(4 \cdot 32 \pm 1 \cdot 5 =) 5 \cdot 82$ and 2·82 m according as the tide is high or low. Thus, mere superposition of surge on tide gives an over-estimate of storm tide in case of high tide and an under-estimate in case of low tide.

4. Concluding remarks

Storm surge generation, like any oceanic or atmospheric event, is a very complex phenomenon and occurs as a result of air/sea/land interaction. The present study is only an attempt to approximate storm surge based on simplified assumptions of straight line (unbroken by bays or estuaries) coast and a vertical wall at the coast. The study does not deal with curved coastline, or with storms that move along shore, recurve, remain stationary, accelerate or with storms whose size varies with time. The pre-computed nomograms to determine the peak surge or total tide are not fully independent. Generally, however, they are weakly inter-related. As such, they can be used to a sufficient degree of accuracy subject to the limitations stated above. The success of storm surge predictions, however, depends on the accuracy of forecasting critical meteorological factors, *e.g.*, the pressure drop, the radius of maximum wind, the storm motion, the landfall point and the time of landfall.

Acknowledgements

The author wishes to place on record his sincere thanks to the World Meteorological Organization, the Governments of India and the United States and the Director General of Observatories of India for providing the opportunity to make this study possible.

He is especially indebted to Dr. Chester P. Jelesnianski for his patient, *ab initio* exposition of storm surge dynamics and invaluable guidance during the course of the study.

He is grateful to Dr. Jye Chen for his every possible help in computer programming and thanks the other personnel of the Marine Techniques Section of TDL for their assistance. Appreciation is extended to Mr. William C. Herrmann for drafting most of the figures.

REFERENCES

Conner, W. C., Kraft, R. H. and Harris, D. L. 1957 *Mon. Weath. Rev.*, **85**, 4, pp. 113-116.

Das, P. K., Sinha, M. C. and Balasubramanyam, V. 1974 *Quart. J. R. Met. Soc.*, **100**, 425, pp. 437-449.

Flierl, G. R. and Robinson, A. R. 1972 *Nature*, **239**, pp. 213-215.

Gray, W. M. 1975 "Tropical Cyclone Genesis", *Atmospheric Science Paper* No. 234, Dept. Atmos. Sci., Colorado State Univ. Fort Collins, Colorado, 121 pp.

Jelesnianski, C. P. 1967 *Mon. Weath. Rev.*, **95**, 11, pp. 740-756.

1972 "SPLASH (Special Program to List Amplitudes of Surges from Hurricanes) I. Landfall Storms, *NOAA Tech. Memo.* NWS TDL-46, Tech. Dev. Lab, Nat. Weath. Service, NOAA, Wash. D.C., 52. pp.

U. S. Dep. of Commerce 1974 Tide Tables, High and Low Water Predictions, 1975, Central and Western Pacific Ocean and Indian Ocean," NOAA, *Ocean Survey*, 382 pp.